Advanced treatment planning methods for efficient radiation therapy with laser accelerated proton and ion beams

Stefan Schell[a] and Jan J. Wilkens
Department of Radiation Oncology, Technische Universität München, Klinikum Rechts der Isar, Ismaninger Str. 22, 81675 München, Germany

(Received 8 April 2010; revised 29 July 2010; accepted for publication 1 September 2010; published 20 September 2010)

Purpose: Laser plasma acceleration can potentially replace large and expensive cyclotrons or synchrotrons for radiotherapy with protons and ions. On the way toward a clinical implementation, various challenges such as the maximum obtainable energy still remain to be solved. In any case, laser accelerated particles exhibit differences compared to particles from conventional accelerators. They typically have a wide energy spread and the beam is extremely pulsed (i.e., quantized) due to the pulsed nature of the employed lasers. The energy spread leads to depth dose curves that do not show a pristine Bragg peak but a wide high dose area, making precise radiotherapy impossible without an additional energy selection system. Problems with the beam quantization include the limited repetition rate and the number of accelerated particles per laser shot. This number might be too low, which requires a high repetition rate, or it might be too high, which requires an additional fluence selection system to reduce the number of particles. Trying to use laser accelerated particles in a conventional way such as spot scanning leads to long treatment times and a high amount of secondary radiation produced when blocking unwanted particles.

Methods: The authors present methods of beam delivery and treatment planning that are specifically adapted to laser accelerated particles. In general, it is not necessary to fully utilize the energy selection system to create monoenergetic beams for the whole treatment plan. Instead, within wide parts of the target volume, beams with broader energy spectra can be used to simultaneously cover multiple axially adjacent spots of a conventional dose delivery grid as applied in intensity modulated particle therapy. If one laser shot produces too many particles, they can be distributed over a wider area with the help of a scattering foil and a multileaf collimator to cover multiple lateral spot positions at the same time. These methods are called axial and lateral clustering and reduce the number of particles that have to be blocked in the beam delivery system. Furthermore, the optimization routine can be adjusted to reduce the number of dose spots and laser shots. The authors implemented these methods into a research treatment planning system for laser accelerated particles.

Results: The authors' proposed methods can decrease the amount of secondary radiation produced when blocking particles with wrong energies or when reducing the total number of particles from one laser shot. Additionally, caused by the efficient use of the beam, the treatment time is reduced considerably. Both improvements can be achieved without extensively changing the quality of the treatment plan since conventional intensity modulated particle therapy usually includes a certain amount of unused degrees of freedom which can be used to adapt to laser specific properties.

Conclusions: The advanced beam delivery and treatment planning methods reduce the need to have a perfect laser-based accelerator reproducing the properties of conventional accelerators that might not be possible without increasing treatment time and secondary radiation to the patient. The authors show how some of the differences to conventional beams can be overcome and efficiently used for radiation treatment.
[DOI: 10.1118/1.3491406]

Key words: laser particle acceleration, proton beam therapy, ion beam therapy, treatment planning

I. INTRODUCTION

Laser-based particle acceleration shows great promise for the future production of charged particle beams for radiation therapy.[1] Whereas nowadays large and expensive cyclotrons or synchrotrons are used to accelerate protons or carbon ions, the mechanism of laser plasma acceleration might potentially reduce the overall costs in particle therapy. This could allow a widespread use of the superior properties of protons and ions compared to conventional x-ray radiation. However, much research need to be performed until a commercial laser accelerated treatment device will be available off-the-shelf.[2] Currently, the most pressing problem is the particle energy. Up to now it is not high enough for the treatment of patients, but there is hope that this is obtainable in the near future.[3]

As soon as the required energies (up to 250 MeV for protons and 400 MeV/u for carbon ions) for radiation treat-

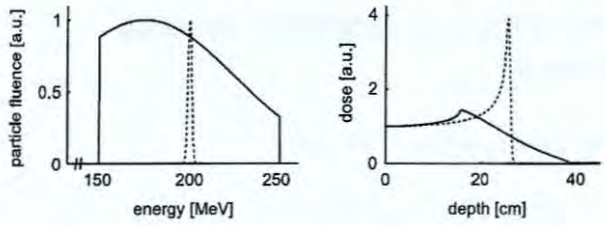

FIG. 1. Energy spectrum (left) and corresponding depth dose curve (right) for conventionally accelerated (dashed line) and laser accelerated (solid line) proton beams. Spectra are normalized to the maximum. Depth dose curves are normalized to equal entrance doses.

ment are available, further problems will have to be solved. The first one is the energy spectrum of the particle beam. Conventional accelerators produce a sharp energy with only little spread, which gives rise to the sharp Bragg peak in the depth dose curve. Laser accelerated particle beams on the other hand are currently not monoenergetic and will probably never be as monoenergetic as the ones from cyclotrons or synchrotrons.[4] Furthermore, since the laser itself is pulsed, the particle beam is pulsed, too. Therefore, two additional important properties of the machine have to be taken into account: The repetition rate of the laser and the number of accelerated particles per shot. Both values have to be within certain limits to enable treatment.

The purpose of this work is to deal with these (currently unknown) machine properties from the point of view of treatment planning. The question we want to answer is: What are the possibilities and limitations for treatment planning given by nonmonoenergetic energy spectra, the repetition rate of the laser, and the number of particles per laser shot? We present advanced methods of treatment planning that are adapted for laser-based particle accelerators. Simply trying to use particles from these machines in a conventional way (such as spot scanning) could work but might not be the most efficient way of performing the treatment with respect to both treatment time and dose burden to the patient due to secondary radiation (e.g., neutrons). The proposed methods include simultaneous irradiation of axial or lateral spot neighbors within the target, which is called *clustering*. Additionally, the conventional optimization routines are modified to respect laser specific optimization goals. Since our treatment planning methods require a special hardware setup (i.e., dose delivery system), we will also describe the requirements for these parts of the machine. However, the focus will be on treatment planning and therefore we will not elaborate on the setup in detail.

II. MATERIALS AND METHODS

II.A. Description of laser properties and consequences for treatment

We want to concentrate on three properties of laser accelerated particles that have an important impact on treatment planning: Energy spectrum, repetition rate, and number of particles per laser shot. The consequence of the first one, the energy spectrum, is depicted in Fig. 1. The spectrum of laser accelerated particle beams depends on the specific laser setup and it is not known yet which spectra will be available for clinical implementation. As of today, experimentally observed spectra typically contain a broad range of energies with an exponential decay toward high energies due to the nature of acceleration. There is hope that a regime can be found that produces a maximum in the spectrum at a well-defined high energy,[3,5–7] which might eventually lead to nearly monoenergetic spectra. While this is certainly very attractive for therapy, these beams might have the problem that the number of accelerated particles per shot is much higher than desired and that some means to reduce the fluence will be necessary. In the meantime, we still have to work with relatively broad spectra and the one used in the figure is a somewhat arbitrary example illustrating the differences compared to the monoenergetic case of conventional accelerators.[8,9] Both depth dose curves show a maximum at a well-defined depth, but the one of laser accelerated particles is not very distinct since the peak is lower and the distal dose decline extends over several centimeters (depending on the width of the incoming spectrum). This is because particles with different energies have their Bragg peak at different positions in the irradiated tissue. To be able to perform precise radiation therapy with broad spectra, a device to select particles based on their energy is necessary (see Sec. II B 1).

The next property, the repetition rate, is important since treatment time is limited. If the particle number per shot were just right for every shot, the number of irradiated spots would give an estimate of how many shots are needed to cover the target with dose. In intensity modulated particle therapy (IMPT), the number of spots is typically at least of the order of 10^3, which gives a lower limit on the repetition rate of 10 Hz to be able to perform a treatment within a few minutes. Because it will be very hard to deliver exactly as many particles per shot as needed to receive the prescribed dose, the number of shots per spot will be higher in general.

The remaining property is the number of particles per laser shot. If it is too low, many shots will have to be placed at each spot, which could lead to problems with repetition rate (and thus treatment time). On the other hand, if it is too high, there will have to be a system that removes some particles from the beam to prevent overdosage (see Sec. II B 2).

Figure 2 gives an overview of different cases subject to the details of the acceleration machine. The treatment possibilities depend on the parameters mentioned above. This illustrates that some settings will not work for conventional treatment methods such as spot scanning. Especially, the repetition rate is an important factor that could render the treatment impossible. In addition to the limits discussed above, there are further requirements for laser accelerated particles to find their way into radiation therapy. The beam needs to be well-defined and reproducible with regards to the energy spectrum, the number of particles, and the emittance angle, which we assume as granted for the purpose of this work.

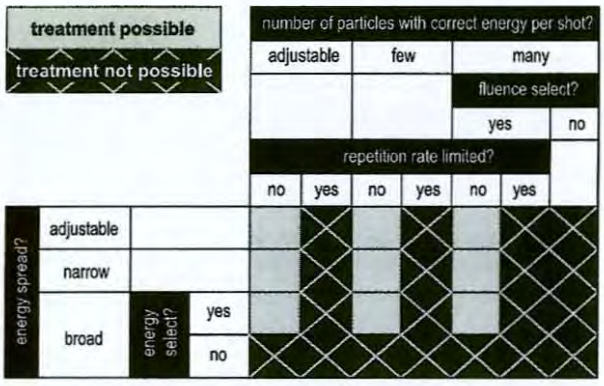

FIG. 2. Overview of different cases for the properties of a particle beam produced by laser acceleration and their impact on radiation therapy. *Energy select* refers to presence of an energy selection system; *fluence select* refers to a fluence selection system.

II.B. Requirements for advanced treatment methods

II.B.1. Energy selection system

Figure 3 shows a schematic example of a setup to perform radiation therapy with laser accelerated particles. As already mentioned, a system to select particles based on their energy will be required. Fourkal *et al.*[10,11] proposed a setup that magnetically bends particle tracks depending on their energy and then blocks the ones with unwanted energies. For the methods presented below, the window of transmitted energies must be adjustable on a shot to shot basis. Blocked particles will produce secondary radiation (in particular neutrons) which has to be shielded.[12] This secondary radiation will most likely be generated very close to the patient since the full potential of laser accelerated particle beams in terms of cost reduction can only be utilized if a compact gantry structure is constructed. This gantry would contain mirrors to guide the laser rather than heavy bending magnets and the laser plasma interaction would take place in the treatment room itself. A treatment planning strategy that uses as many of the accelerated particles as possible will reduce the number of particles that have to be blocked within the energy selection system. In the following, we will talk about increased *axial particle efficiency* to describe cases where fewer particles are blocked. We call this quantity *axial* particle efficiency since particles with different energies stop at different positions along the beam axis. To quantify the efficiency, the number of blocked particles or the total blocked energy can be used. The energy selection system described so far can only choose between energies that are transmitted or not. It cannot change the number of particles per energy bin. In our earlier work,[13] we showed that an additional scattering material within the transmission window can change the number of particles per energy bin in a way that naturally produces spread out Bragg peaks (SOBPs) within one shot. However, to keep the setup simple, we do not use this possibility in the following. Since the laser might not be able to produce particles with all the required energies (or at least not with the required efficiency), an additional range shifter might be necessary to slow down higher energy particles (Fig. 3).

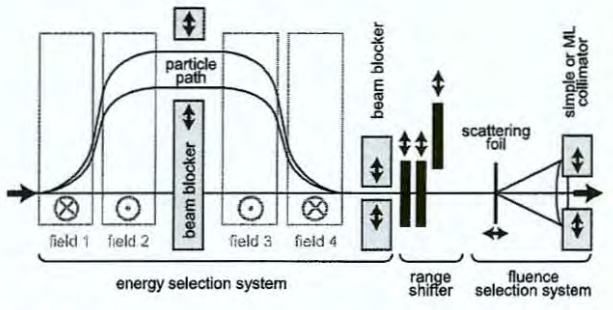

FIG. 3. Schematic drawing of a beam delivery system to perform radiation therapy with laser accelerated particles. The beam delivery system consists of the magnetic energy selection system, the range shifter, and the fluence selection system. The latter can contain a simple or a multileaf collimator. Particles enter the system from the left and reach the patient on the right hand side.

II.B.2. Fluence selection system

Since all particles from one laser shot are expelled within nanoseconds, it is not possible to use active beam shutters to remove surplus particles from the beam or to use magnetic scanning within one shot. One way to reduce the resulting fluence is a scattering foil with a subsequent collimator. If the collimator is at a fixed position and the scatterer can be moved upstream and downstream relative to the beam, the number of transmitted particles can be chosen. Furthermore, if the collimator itself can be opened and closed, the lateral beam spot size can be adjusted as well. This collimator could even be a multileaf collimator (MLC) to irradiate irregular beam spots, although in this case a double scattering system might be better than a single scatterer to achieve a homogeneous fluence across the field. It depends on the details of the particle acceleration whether or not a MLC is useful for a given irradiation (see below). Independent from the actual technical implementation, a setup like this will again lead to an increase in secondary radiation. Following the convention from above, a laser shot has a high *lateral particle efficiency* if the fluence selection system can leave many particles within the beam.

II.C. Advanced treatment planning methods

II.C.1. Clustering

Dose delivery is usually planned by employing a virtual three-dimensional grid within the patient. To transport dose to each of the grid points within the planning target volume, in the axial direction (measured in radiological depth, see Ref. 14) the energy has to be chosen correctly and in the lateral direction a magnetic scanning system or a collimator is used. Figure 4 shows the principal idea of clustering. Conventional spot scanning irradiates each target spot in the dose delivery grid independently (case A) with exactly the number of particles that is required.[15] This kind of dose delivery provides a huge number of degrees of freedom and is an excellent way to deliver the dose with conventionally accelerated protons or ions. However, this might be impossible

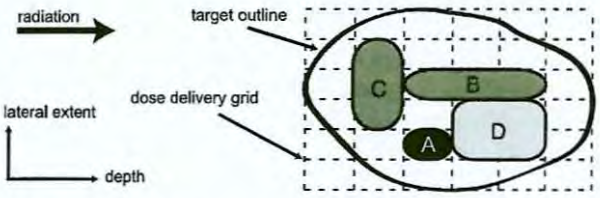

FIG. 4. Clustering of dose spots. The whole target has to be covered with dose. There are several possibilities how to treat the individual spots. A: Conventional dose spot, B: Axial clustering, C: Lateral clustering, and D: Clustering in both directions.

FIG. 6. Treatment and decay area of a depth dose curve as used by our algorithm to place differently broad energy spectra within the target.

with laser accelerated ions due to the limitations mentioned above. Clustering means that not all spots are irradiated independently (cases B–D). We will show that it is possible to provide a good treatment plan with a reduced number of degrees of freedom. Some spots can be grouped together and some are kept independent (see below).

II.C.1.a. Axial. Axial clustering tries to minimize the disadvantages occurring because the laser produces more than one ion energy simultaneously. Since each energy corresponds to a certain depth in the irradiated tissue, the dose deposition of a broad energy spectrum is stretched over a wider axial length compared to monoenergetic beams. The high dose area of a depth dose curve is not limited to only one dose spot of the conventional dose delivery grid. Figure 5 shows an example of how a SOBP can be built by adding laser shots with *different spectral widths*. The decision of where to cluster spots and where to keep them independent is done before the treatment plan optimization is started. Hence, when optimizing the fluences, the clusters are kept constant. The cluster search algorithm can be applied independently of the form of the energy spectrum. It only needs to know the depth dose curves of all available settings of the energy transmission window. Settings are given by their mean transmitted energies and the widths of the transmitted spectra. For each depth to be irradiated, a subset of possible transmission window settings that reach this spot with their Bragg peak is compiled. The algorithm iterates over all target depths of each pencil beam (i.e., each ray from the source passing through the target on a predefined lateral grid). The aim is to cover the whole target with laser shots of maximal beam efficiency (maximal ion energy spread) with the constraint of no relevant dose behind the distal target edge.

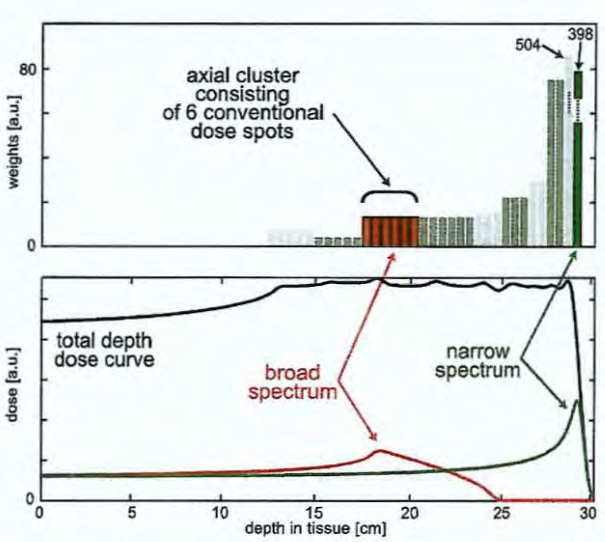

FIG. 5. Spot weights and depth dose curve for axial clustering. Adding the depth dose curves of various wide energy spectra builds up a SOBP. For the proximal and middle parts of the target, broad energy spectra can be used (high axial particle efficiency, low number of independent dose spots). They cover several conventional dose spots that are clustered into one spot. Only the distal edge requires narrow energy spectra (sharp dose decline). In this example, 34 conventional spots are replaced by ten spots.

In detail, the algorithm identifies two areas within each depth dose curve (see Fig. 6). The first one is the *treatment area* where the dose is high enough for treatment (in our simulation, this is set to the area with more than 80% of the maximum). If the target has a sufficient axial extension, all depth spots within the treatment area are clustered into one new spot that is irradiated with one machine setting. If the target extension is smaller than the treatment area, a smaller energy transmission window is applied. If this were the only criterion, the distal dose decline would be very long. The algorithm needs another measure to ensure that this does not happen. Therefore, a second area of the depth dose curve is defined. It is called *decay area*, which is the area downstream of the treatment area where the dose is still quite high [we use the depth from 80% (distal) down to 20% of the maximum]. Dose spots in this area are not clustered together with the ones in the treatment area but will primarily be irradiated by the neighboring dose spot (with an energy window of higher mean energy). The additional criterion that ensures a steep distal dose decline is that for the use of a specific transmission window, the decay area has to be completely located within the target. Otherwise, a narrower setting is used. For illustration, Fig. 7 shows an exemplary pencil beam where eight spots (labeled 1–8) are part of the planning target volume (PTV). For this example, let us assume that we only have one ion range available in the spectrum but various energies spread around this range. We shift the beam in depth with a range shifter. Therefore, the list of available depth dose curves (resulting from various energy spreads) is the same for every dose spot (in general each depth has its own list of possible settings). The depth dose curves can be described by the extent of the treatment area and the extent of the decay area, both lengths given in multiples of the spot spacing. For example, 6+3 means that the

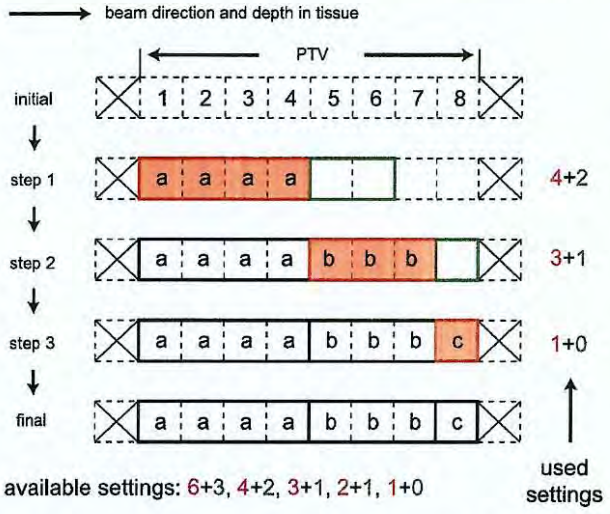

FIG. 7. Example for the application of the axial clustering algorithm. Starting upstream, several steps (in this case, three) are used to find appropriate clusters. The scheme $x+y$ means that, in multiples of the spot spacing, the treatment area is x units and the decay area is y units wide. Only curves with both treatment and decay area within the tumor are allowed. The available settings are sorted by beam efficiency and sampled according to this sequence. See text for further details.

treatment area extends over six spots and the decay area over three spots. Our list of possibilities for each depth shall be 6+3, 4+2, 3+1, 2+1, and 1+0. This list is sorted by beam efficiency. Initially, the eight spots are not assigned to any cluster. In step one the first cluster is built. There are only eight PTV spots. Since both treatment and decay area have to be within the PTV, the 6+3 curve does not fit. The first appropriate option is the 4+2 curve which is placed in the proximal part of the PTV. Hence, spots 1–4 are put into cluster "a." The decay area covers the following two spots; however, these are within the tumor and the dose does no harm to the surrounding tissue. In the second step, the next cluster is formed downstream of cluster a. We search for the most efficient transmission window setting that can be used to irradiate spots beginning with number 5. Note that here we place a spot in the decay area of the spot further upstream. The best choice for this spot is the 3+1 setting, creating cluster "b" from depths 5 to 7 with a decay area reaching to depth 8 only. Then, the last step has no other option than to use the smallest available transmission window setting producing depth dose curve 1+0 to create the last cluster ("c") with just one member (depth 8). For the general case of different depth dose curves for each depth (no range shifter necessary), the algorithm has to apply the actual depth dose curve corresponding to the current spot. Since we use absolute energy spreads for the different transmission window settings, this can result in slightly bigger clusters downstream in the beam (the range increases faster than linear with ion energy[16]). This can be seen in Fig. 5 where the first two clusters consist of five spots each and the third one extends over six spots. Here, all three clusters use the same absolute transmission window width but different mean energies.

As a consequence of the presented clustering strategy, at the proximal edge and in the middle of the target, several depths can be combined into one cluster that is irradiated with a broad energy window. This reduces the number of independently irradiated dose spots and increases the axial particle efficiency. For these spots, it does not matter that the decay area of the broad energy spectra is quite long since there is plenty of target downstream of the spot that needs dose anyway. At the distal edge, no clustering is possible and smaller settings of the energy window are used instead. For monoenergetic beams, both the treatment and the decay areas are very short. As a result, if only narrow energy spectra are available (conventional acceleration method), the algorithm described above will produce dose spots at the positions of a conventional dose delivery grid.

II.C.1.b. Lateral. Lateral clustering is useful if the number of particles per shot within a relatively narrow energy window is very high. Instead of throwing away a certain percentage of particles, they can be spread over a bigger lateral area. As described above, the fluence selection system can be used to irradiate a bigger lateral area. If the collimator is a MLC, the shape of this area can be varied. We investigated two different possibilities of lateral clustering: *Prior* lateral clustering and *posterior* lateral clustering. The difference is the time within treatment planning when the clustering is performed.

Prior lateral clustering means that it is done before the treatment plan optimization. It is based on geometrical considerations only. For each isoenergy slice (i.e., for constant radiological depth), neighboring target spots on a predefined lateral grid can be clustered up to a certain cluster size. However, to enable a good treatment plan with sharp lateral gradients, points on the edge of the target should not be clustered.

Our algorithm of choice for this work is posterior lateral clustering which is performed after the optimization has been done (similar to leaf sequencing as a postprocessing step in intensity modulated radiotherapy with photons). The spots are kept independent during the (first) optimization to allow the best possible treatment plan. After this optimization is finished, the resulting spot weights for each energy setting are compared to each other. We use a modified version of a standard "k-means" clustering algorithm (for an overview, see Ref. 17) in combination with a neighborhood clustering algorithm to find lateral neighbors that have similar weights (which, for example, do not differ by more than 20%). The first requirement for clustering is that the spots are locally connected to each other. This ensures that a MLC can be used to form the cluster. The second requirement is that all spots use the same energy setting. Within each of these possible groups, the k-means algorithm then tries to identify the smallest possible number of subgroups that have similar spot weights. It starts with $k=1$ and increases its size until the similarity criterion (for example, at most 20% difference) is fulfilled for all group members. These subgroups are merged

into new nonoverlapping dose spots and the optimization is restarted. The whole procedure is repeated several times (usually two cluster searches, each with a consecutive reoptimization).

Prior and posterior lateral clustering can be combined depending on the requirements of the individual treatment plan. Apparently, it makes a difference *how much* clustering is done but not *when* it is done. As a side remark, we want to add that lateral clustering is an irradiation method that is somewhere between two well known methods; the extreme cases are no clustering which is spot scanning and full clustering which is layer stacking.[18,19] Clustering parameters control how close the result is to either of these methods.

II.C.1.c. Axial and lateral. We have described how axial and lateral clustering work in detail. In principle, both methods can be applied simultaneously to create a treatment plan. However, they are not independent from each other. The three-dimensional dose spots given by axial clustering in the depth direction and lateral clustering in the lateral direction are cuboids. Clustering can only be done if the energy selection system is set to the same transmission window for all participating lateral spots. In general, it is not clear how to cover an arbitrary target volume with differently sized cuboids since there must be a priority concerning which clustering direction is more important. We implemented a procedure to synchronize both methods in a way that makes clustering in both directions easier; however, this problem has not been fully solved yet. The current approach tries to look at multiple adjacent pencil beams simultaneously to increase the likelihood that neighboring pencil beams use the same energy transmission window setting in as many depths as possible. If in one pencil beam a highly efficient beam spot has been placed in a given depth, the axial cluster search in the neighboring pencil beams is not started at the upstream end of the PTV but at the depth where the efficient spot of its neighbor begins. The remaining upstream spots are processed afterward. Our approach is to start the procedure with the pencil beam that has the widest PTV. This synchronization attempt causes a slightly decreased beam efficiency for axial clustering but increases the efficiency of lateral clustering.

II.C.2. Modification of the optimization

So far we have concentrated on alternative methods of dose delivery for laser accelerated particle therapy. The focus of Sec. II C 2 is on changes to the optimization algorithm that help minimize laser specific disadvantages. The starting point in our considerations is the usual quadratic objective function F_0 for the actual doses D_i and the prescribed doses D_i^0 in all voxels that is used in many treatment planning tools[20]

$$F_0(\vec{\omega}) = \sum_{\text{voxels } i} (D_i(\vec{\omega}) - D_i^0)^2. \quad (1)$$

Here, the spot weights $\vec{\omega}$ determine the dose and are varied to minimize F_0. For laser accelerated particle therapy, the weights can be scaled to equal the required number of laser shots.

II.C.2.a. Reduce number of shots. Since the repetition rate of the laser is certainly a limit for radiation therapy with laser accelerated particles, it is desirable to keep the number of required shots as low as possible ($\min \Sigma_j \omega_j$). This can be achieved with several methods. The first and easiest one is to add an additional term to the usual objective function

$$F(\vec{\omega}) = F_0(\vec{\omega}) + p \sum_j \omega_j. \quad (2)$$

The penalty factor p can be chosen automatically by doing an intermediate optimization of F_0 first and then setting p, such that the additional term in F with the intermediate weights has a certain magnitude (we use 0.1%) compared to the intermediate value of F_0.

The second method is the use of hard constraints for the minimization of F_0. This requires a rough estimate of how many shots one needs and how many are allowed. The algorithm will guarantee that not more than a given number of shots are used but will not try to reduce it further. Last but not least, there is a third possibility. In prioritized optimization (see Ref. 21), the first step is the minimization of F_0. Based on this result, certain hard constraints can be deduced for a second optimization step that minimizes the number of shots as the only criterion. A possible constraint is that the value of F_0 does not increase above a certain level compared to the first step. In the following, we will concentrate on the first method (additive term) since it proved to be most practicable.

II.C.2.b. Reduce number of spots. To reduce treatment time, not only the number of shots but also the number of spots is relevant. When using a MLC to shape the dose laterally, the number of spots must not be much higher than 1000 (if the MLC needs 1 s to align, this would already mean a time of more than 15 min). Even if no MLC is used, the reduction of dose spots will certainly save time. This problem is already approached with clustering of dose spots which reduces the number of independent spots. However, the number can be decreased further by using repeated runs of the optimization. After one run, the spots that do not contribute to the integral target dose to more than a certain level compared to the average target dose contribution for all spots are removed completely. Afterward, the optimization is started again. We remove spots twice (with a subsequent reoptimization after each removal) and set the limit to remove the spots to 10% of the average spot contribution to the target. This procedure can remove many redundant dose spots (degrees of freedom) without changing the quality of the treatment plan (see below).

II.C.2.c. Shot numbers are integers. The number of laser shots that can be delivered is a natural number. Since integer programing is more complicated and much slower than optimization with real numbers, we stick to the usual algorithms for the optimization part.[22] Nevertheless, we include the quantization of the number of shots into the system as much as possible. After the optimization has been performed, each spot weight is analyzed. Some can be rounded toward

the nearest integer without changing the resulting dose distribution very much (if the relative change of the weight is below 10%). Some other spots can be rounded to 0 (below 10^{-3}). All others cannot be rounded without changing the plan. The fluence selection system has to be used for the last shot of these spots. This decreases the lateral particle efficiency. We fully understand that at this point, integer programing could provide a better solution in some special cases. However, the problematic cases are the ones with only few (or even just one) shots per spot. For these the problem of too many particles per shot persists.

II.D. Implementation in treatment planning system

To investigate the methods presented so far, we implemented a simulation framework for laser accelerated proton therapy into a treatment planning system. The methods are independent of the actual particle type and are therefore applicable for protons and heavier ions. However, the actual calculations have all been performed for protons. The implementation is based on the Computational Environment for Radiotherapy Research,[23] which is an open source radiotherapy tool written in MATLAB (www.mathworks.com). It allows loading of CT images, region of interest contouring, dose calculation for photons, treatment plan optimization, and treatment plan analysis. We added the capability to calculate dose distributions for proton beams of arbitrary energy spectra. This is done by decomposition into monoenergetic beams that can be simulated with the help of lookup tables or an analytical approximation for the depth dose curve[16] and the lateral spread.[24] We use a simple finite pencil beam algorithm (for an overview about pencil beam algorithms, see Ref. 25) since the kind of problems we want to analyze do not depend on tissue heterogeneities. We distinguish between Gaussian-shaped spot scanning dose delivery and the delivery with radiation fields defined by a MLC. If lateral clustering is not used, for particle efficiency reasons no MLC is applied but a conventional spot scanning beam. There is always a reduced lateral particle efficiency for a MLC since a usually circular beam must be collimated by a rectangular field shape. We included this loss of efficiency in our algorithm. Since the optimization problems in the simulation are quadratic both within the objective function and the constraints, we use MOSEK (www.mosek.com) as a commercial optimization routine for all optimization tasks.

III. RESULTS

In the following, we present treatment planning studies that apply our proposed methods. They show that laser accelerated particles plans with increased efficiency compared to the "conventional" methods can be created without sacrificing the plan quality. We describe the impact on treatment planning for each of these methods. As an illustration, a head and neck case containing a tumor close to the left parotid gland is used. It is treated with two coplanar intensity modulated proton beams. Both the lateral dose spot spacing (in the isocenter) and the axial dose spot spacing (radiological depth) are 5 mm before clustering. This forms the conventional dose delivery grid. Because of the dose quantization, the plan has to be calculated based on the dose per fraction (2 Gy prescribed dose) and not for the whole course. The most important volumes of interest (VOIs) are the *ipsilateral parotid gland* and the PTV (volume: 285 cm^3). The third VOI (called *PTV shell*) is a volume of 1 cm thickness that surrounds the PTV. The lower the dose in this volume, the steeper are the dose gradients between PTV and normal tissue. The PTV shell is used for both optimization and visualization of these dose gradients around the PTV.

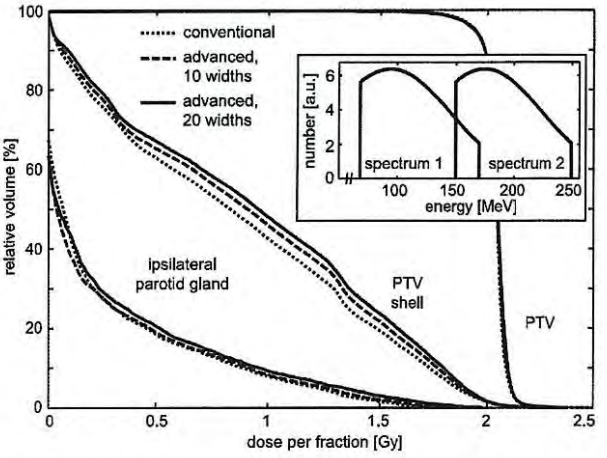

FIG. 8. Axial clustering for a head and neck case. The inset shows the available energy spectra from the laser-based accelerator. These spectra are used to produce the conventional plan (spot scanning, no clustering, energy transmission window set to 1 MeV in width, no modification of optimization) and the advanced plans [axial clustering, 10 (20) energy transmission window settings from 1 to 10 (20) MeV in width, modified optimization]. The advanced plans need approximately 43% (35%) of the spots and 12% (8%) of the shots while producing 11% (7%) of the amount of secondary radiation compared to the conventional plan.

III.A. Case studies for clustering

III.A.1. Axial clustering: Broad energy spectra

The first example is a study where the laser acceleration device produces energy spectra of great width. In Fig. 8 we simulate the case that two spectra of different mean energy can be produced on demand (see inset). The total number of particles per shot is 10^8. Again, these spectra are not from measurements but they are similar to what could be available in the future. A broad beam from spectrum 1 with a fluence of 10^8 particles per spot (0.25 cm^2) results in a peak dose of 1.4 Gy in a depth of 4.1 cm. For an only 20 MeV wide part around the maximum of the spectrum, this value is reduced to 0.63 Gy in a depth of 5.8 cm. We calculated three plans: The first one is a standard spot scanning plan where the energy selection system cuts monoenergetic beams (1 MeV wide) out of the total spectrum (conventional: No clustering, no MLC). It uses 3665 spots and 68 064 shots. A total energy of 129 J has to be blocked within the energy selection system. The two advanced plans use the spot scanning technique with axial clustering (no lateral clustering, no MLC) and differ in the number of available widths for the energy trans-

mission window. One uses ten equispaced steps from 1 to 10 MeV and the other uses 20 equispaced steps from 1 to 20 MeV. We turned on the modification of the objective function (additive term) to decrease the number of shots and also activated the removal of unnecessary dose spots. These plans only need 1586 (1298) spots (plan with ten and 20 widths, respectively), which is 43% (35%) compared to the conventional plan. The shot number is 8014 (5538) or 12% (8%) of the conventional plan and the blocked energy is 15 J (10 J), which is 11% (7%) of the conventional plan. Thus, the efficiency of the system regarding time and secondary radiation is much higher, approximately by a factor of 9 (14). In the dose volume histograms (DVHs), the ipsilateral parotid gland and the PTV do not show any relevant difference. There is slightly more dose in the PTV shell for the advanced cases. There are two main reasons for the increase in dose. First, there are fewer degrees of freedom and second, the algorithm for placing beams with differently sized energy spectra within the PTV allows spot combinations that have 20% dose behind the distal edge of the PTV (beyond the decay area, see above). This setting could be changed; however, at some point, we need to find a compromise between plan quality and treatment practicability.

The case discussed above uses two beams that are optimized simultaneously. The IMPT technique is favorable for axial clustering since in this case, not all PTV spots along a pencil beam have to be irradiated to the same extent to form a flat depth dose curve within the tumor. The distal spots of one pencil beam that cannot be merged very efficiently because of the long decay areas of bigger clusters might easily be clustered when using another beam direction. Therefore, the optimization can use the direction that is most efficient. However, the clustering technique also works when applying single beam optimization. We created treatment plans with the same settings as above that use only one beam instead of two. The DVHs for the conventional plan and the advanced plan (using 20 different energy widths from 1 to 20 MeV) are again comparable (not shown). Here, the spot number could be reduced to 36% and the shot number to 11% compared to the conventional plan. The axially blocked energy is lowered to 13% which is of course not as efficient as the 7% we found for the plan with two beams. Figure 5 shown above is obtained by irradiating a water phantom with a SOBP. The pencil beams from the patient plan using just one beam are equivalent to this. There is a certain amount of fluence to dose spots at the distal edge that cannot be clustered. In contrast to this, the plan with multiple beams avoids dose to the distal edge and irradiates this area from another direction. This is due to the modifications to the objective function which try to minimize the number of shots and therefore increase the usage of highly efficient dose spots. However, this is achieved by using different spot weights only; the cluster pattern itself is not changed since it is performed for each beam independently.

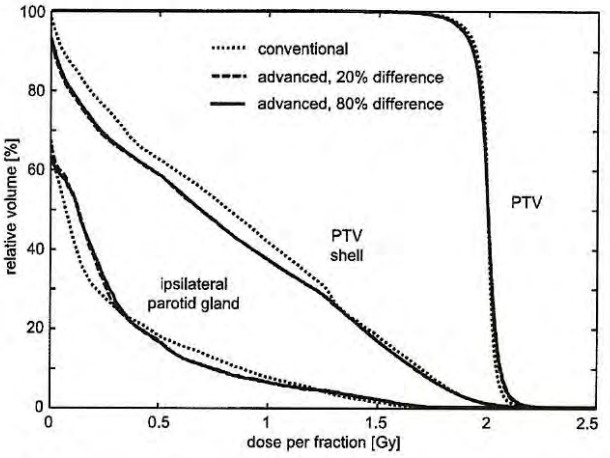

FIG. 9. Lateral clustering for a head and neck case. Comparison of conventional plan (spot scanning, no clustering, no modification of optimization) with two advanced plans (with MLC, modified optimization) using posterior lateral clustering of neighbors that differ up to 20% (80%) in weight. The advanced plans need approximately 80% (55%) of the spots and 80% (55%) of the shots while producing 84% (58%) of the amount of secondary radiation compared to the conventional plan.

III.A.2. Lateral clustering: High number of particles per shot

Figure 9 shows the application of lateral clustering in the same patient case. We assume a broad energy spectrum in combination with a narrow setting of the energy selection system which transmits 6×10^8 monoenergetic particles per shot for every required energy. For the analysis of lateral clustering this is equivalent to a (tunable) monoenergetic beam. Since more particles per energy than needed are available in every shot, some of them have to be removed by the fluence selection system. For example, a broad beam with 200 MeV and a fluence of 6×10^8 particles per spot (0.25 cm^2) would produce a dose of 18 Gy at a depth of 25.8 cm.

The first plan uses a conventional spot scanning technique in which the number of particles is reduced with an additional beam spreading foil and a subsequent circular collimator of fixed size. It needs 3422 spots and the same number of shots. A total energy of 35 J has to be removed from the beam within the fluence selection system. The two advanced plans which employ a MLC instead of a simple collimator apply posterior lateral clustering of neighbors which differ up to 20% (80%) in their weights. As already mentioned, this clustering is done twice, leading to a total number of three executions of the optimization routine for each plan. Additionally, the number of spots and shots is reduced as described above. These plans get along with 2740 (1873) spots, which is 80% (55%) compared to the conventional plan and 2741 (1888) shots [80% (55%)]. The removed energy amounts to 30 J (20 J) or 84% (58%) of the conventional plan. In this comparison, some differences can be seen in the DVHs. There is less dose in the PTV shell for the advanced plans. This is due to fewer effects originating from the rounding of spot weights to integers. Instead of rounding, the

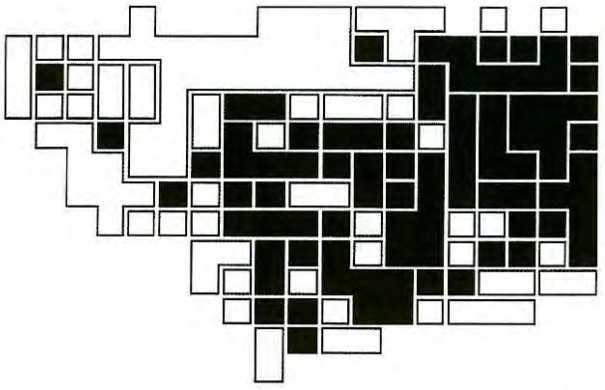

FIG. 10. Typical isoenergy slice of the advanced treatment plan (called 80% *difference* in Fig. 9) illustrating lateral clustering. There are 175 spots in total; 74 of them are independent and the remaining spots are clustered into 30 different groups. Filled boxes are irradiated with a certain dose and empty boxes denote spots whose weights have been set to zero within the optimization. The great amount of spots with zero dose is caused by the modifications to the objective function which try to minimize the number of spots.

fluence selection system could be used in more cases; however, this would further decrease the efficiency. The low dose part of the ipsilateral parotid glands receives more dose when using a MLC. As an illustration, Fig. 10 shows the cluster pattern of a typical isoenergy slice of the advanced plan where neighboring spots which differ up to 80% are merged.

III.A.3. Simultaneous axial and lateral clustering

Last but not least, we present a case with a broad energy spectrum *and* many particles per energy bin. The spectrum is the one from the axial case (see inset of Fig. 8) but now with a total number of 10^9 particles per shot. Figure 11 compares a conventional plan (no clustering, no modification of optimization) with an advanced plan which uses both axial and (posterior) lateral clustering simultaneously (modified optimization). To increase the flexibility for simultaneous axial and lateral clustering, only three different widths of the energy transmission window are allowed (1, 5, and 10 MeV). Two steps of posterior lateral clustering are performed for neighboring spots whose weights differ by up to 20%. The advanced plan uses only 50% of the spots and 31% of the shots, while the energy blocked in the energy selection system is reduced to 31%. On the other hand, the energy blocked in the fluence selection system increased to 997% compared to the conventional plan. This shows that in some cases, axial clustering can *decrease* the lateral efficiency. However, the *total* amount of energy blocked in the energy and fluence selection systems (and hence the amount of secondary radiation) is reduced to 33%. Nevertheless, the total efficiency cannot be increased as much as in the case of axial clustering only.

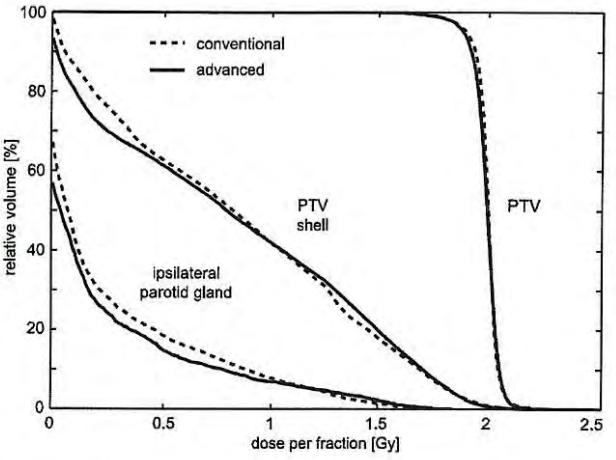

FIG. 11. Axial and lateral clustering for a head and neck case. Comparison of a conventional plan using spot scanning (no clustering, no objective function modification) with an advanced plan using a MLC (axial and lateral clustering, modified objective function). The advanced plan needs 50% of the spots and 31% of the shots while producing 31% of the amount of secondary radiation in the energy selection system and 997% in the fluence selection system compared to the conventional plan. Since the number of laterally removed particles is very low compared to the axially removed ones, the total amount of secondary radiation is reduced to 33%.

III.B. Case studies for the modification of the optimization

So far the focus of our analysis has been on clustering techniques. In the following, we illustrate the modification of the optimization independently from clustering. As described above, we remove spots if they do not contribute high enough to the PTV and restart the optimization. Furthermore, an additional term in the objective function reduces the total number of shots. Figure 12 shows that the reduction of both spots and shots can be done with almost no changes in the

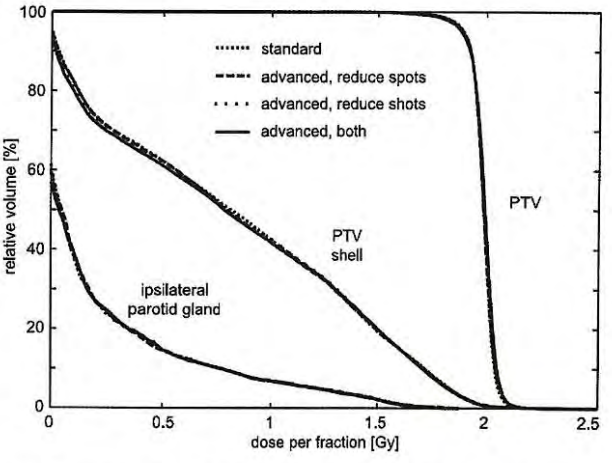

FIG. 12. Modification of the optimization for a head and neck case. All plans were clustered axially and laterally. They only differ in the additional methods to reduce the number of spots and shots. Standard: 2435 spots with nonzero weight, 4414 shots; advanced, reduce spots: 1874 nonzero spots (77%), 3958 shots; advanced, reduce shots: 2349 nonzero spots, 2907 shots (66%); advanced, both: 1796 nonzero spots (74%), 2365 shots (54%).

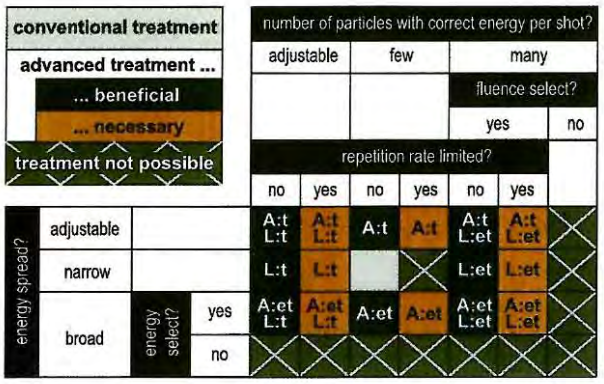

FIG. 13. Overview of different cases for the properties of a particle beam produced by laser acceleration and the possible application of advanced methods in dose delivery and treatment planning. The applicable methods are axial (A) and lateral (L) clustering. Additional changes to the objective function can be applied but are not mentioned here. The reasons for using clustering are an increase in the axial and/or lateral particle efficiency (e) and a reduction in treatment time (t). Compare to Fig. 2.

treatment plan quality. Axial and lateral particle efficiency is increased. In the plan where both methods are applied, the energy deposition in the energy selection system is only 52% and in the fluence selection system 80% compared to the standard case without modification of the optimization. Here, all plans, including the standard case, use axial and lateral clustering.

IV. DISCUSSION

We have introduced methods to perform treatment planning for laser accelerated particles which differ from conventional accelerated particles in their energy spectrum and the quantization of the beam. Figure 2 has been shown to illustrate that not all possible combinations of the properties of a future laser setup can lead to a working system for radiation therapy. However, the advanced planning methods mentioned above are meant to minimize problems due to these limitations and to perform laser-based particle therapy as effective as possible. Figure 13 shows the same table as above but now includes our advanced methods that can, on the one hand, make cases that already worked with conventional planning and delivery more efficient (labeled *advanced treatment beneficial*) and, on the other hand, make some other cases possible at all (labeled *advanced treatment necessary*). For the last group, we want to point out that we do not provide a *general* solution to the problems with laser accelerated particles. Narrow energy spectra, high repetition rates, and a (relatively) low number of particles per laser shot remain advantageous for radiation therapy. However, our proposed methods reduce the need to have the perfect laser setup (which might not be possible). Therefore, the methods can take the system into a region where it is possible to use it for radiation therapy because shielding and treatment time requirements remain feasible.

The developed simulation tool enables us to quantitatively perform treatment planning for various energy spectra and beam quantizations. Based on this, we argue that broad energy spectra can be used in the therapeutic energy range (e.g., between 70 and 250 MeV for protons) in conjunction with an energy selection system if secondary radiation from blocked particles can be shielded sufficiently. Additionally, the number of particles per energy should not change very much within this range (not more than one order of magnitude) to be able to perform the treatment with high efficiency for all required target depths. Given this, with axial clustering, a high number of shots with energy spectra of up to about 20 MeV in width (corresponding to beams with up to 10%–20% energy spread) can be placed within large parts of the target. Of course, this strongly depends on the depth and extension of the target volume.

Regarding the particle number per energy, lateral clustering can increase the efficiency of the system by a certain amount but is not as efficient as axial clustering since the flexibility of intensity modulation is lost when too much clustering is applied. We have not demonstrated results with prior lateral clustering because we found that posterior lateral clustering leads to better results in most of the IMPT cases studied. Prior clustering should provide better results with multiple beams that each deliver a uniform dose. This is because the geometric considerations that lead to the clustering match the boundaries of the beam in this case. Lateral clustering applies concepts of aperture-based optimization as in photon IMRT (see Ref. 26) and can be classified according to the two subfields of this technique. Whereas prior lateral clustering is purely contour-based (since it is done before the optimization starts), posterior lateral clustering uses basic ideas from direct aperture optimization [since the clusters are changed within (or at least after) the optimization]. A full direct aperture optimization approach would certainly yield the best results. We want to point out that lateral clustering in general is only of advantage for a limited range of particle numbers per shot (approximately 10^7–10^9 if monoenergetic). Below this range, no particles need to be blocked and above this range, the total number of particles that have to be blocked is so high that even extreme lateral clustering methods would not change the relative number of blocked particles very much. To further increase the efficiency of the system, a hybrid dose delivery method could be used. Lateral dose spots that are not clustered can be applied with a circular collimator and the clustered ones with a MLC. This avoids the loss of particles when cutting small rectangular fields out of a circular beam.

If the total number of particles in the whole spectrum [e.g., between 70 and 250 MeV, with not too much variation in fluence (see above)] is around 10^8, a repetition rate of 10 Hz might be enough. However, if the particle number is below this, higher repetition rates are required. Further developments in the field of laser plasma acceleration have to show what kind of energy spectra and particle numbers are feasible before the exact specifications for a laser-based particle therapy unit can be made.

V. SUMMARY

The calculations presented in this paper show that laser-based acceleration devices for radiation therapy with protons

and ions have to fulfill certain conditions regarding the energy spectrum, the repetition rate, and the number of particles per shot. However, it is not necessary to reproduce the same beam properties as delivered by classical accelerators (e.g., a very sharp energy spectrum and a quasicontinuous beam). Treatment can also be performed under different conditions and we propose methods to increase the efficiency of the dose delivery system for broad energy spectra and high numbers of particles per shot. Axial clustering utilizes different energies simultaneously and still covers the target with a homogeneous dose. Lateral clustering tries to use as many of the available particles per shot as possible by spreading the beam in the lateral direction and shaping the beam with the help of a MLC. Both of these methods can potentially reduce the treatment time and the amount of secondary radiation that has to be shielded. Additionally, changing the optimization routines in treatment planning can reduce both the number of spots and shots that are necessary to provide a good treatment plan by eliminating some unnecessary degrees of freedom. These measures and considerations can potentially simplify radiation therapy with laser accelerated particles and its clinical implementation.

ACKNOWLEDGMENTS

This work is supported by DFG Cluster of Excellence: Munich-Centre for Advanced Photonics, Grant No. EXC 158.

[a]Electronic mail: stefan.schell@tum.de

[1]C. M. Ma, I. Veltchev, E. Fourkal, J. S. Li, W. Luo, J. Fan, T. Lin, and A. Pollack, "Development of a laser-driven proton accelerator for cancer therapy," Laser Phys. **16**, 639–646 (2006).

[2]U. Linz and J. Alonso, "What will it take for laser driven proton accelerators to be applied to tumor therapy?," Phys. Rev. ST Accel. Beams **10**, 094801 (2007).

[3]T. Tajima, D. Habs, and X. Yan, "Laser acceleration of ions for radiation therapy," Reviews of Accelerator Science and Technology **2**, 201–228 (2009).

[4]S. V. Bulanov and V. S. Khoroshkov, "Feasibility of using laser ion accelerators in proton therapy," Plasma Phys. Rep. **28**, 453–456 (2002).

[5]B. M. Hegelich, B. J. Albright, J. Cobble, K. Flippo, S. Letzring, M. Paffett, H. Ruhl, J. Schreiber, R. K. Schulze, and J. C. Fernández, "Laser acceleration of quasi-monoenergetic MeV ion beams," Nature (London) **439**, 441–444 (2006).

[6]O. Klimo, J. Psikal, and J. Limpouch, "Monoenergetic ion beams from ultrathin foils irradiated by ultrahigh-contrast circularly polarized laser pulses," Phys. Rev. ST Accel. Beams **11**, 031301 (2008).

[7]A. Henig, S. Steinke, M. Schnürer, T. Sokollik, R. Hörlein, D. Kiefer, D. Jung, J. Schreiber, B. M. Hegelich, X. Q. Yan, J. Meyer-ter Vehn, T. Tajima, P. V. Nickles, W. Sandner, and D. Habs, "Radiation-pressure acceleration of ion beams driven by circularly polarized laser pulses," Phys. Rev. Lett. **103**, 245003 (2009).

[8]J. Weichsel, T. Fuchs, E. Lefebvre, E. d'Humières, and U. Oelfke, "Spectral features of laser-accelerated protons for radiotherapy applications," Phys. Med. Biol. **53**, 4383–4397 (2008).

[9]E. Fourkal, I. Velchev, J. Fan, W. Luo, and C. M. Ma, "Energy optimization procedure for treatment planning with laser-accelerated protons," Med. Phys. **34**, 577–584 (2007).

[10]E. Fourkal, J. S. Li, M. Ding, T. Tajima, and C. M. Ma, "Particle selection for laser-accelerated proton therapy feasibility study," Med. Phys. **30**, 1660–1670 (2003).

[11]E. Fourkal, J. S. Li, W. Xiong, A. Nahum, and C. M. Ma, "Intensity modulated radiation therapy using laser-accelerated protons: A Monte Carlo dosimetric study," Phys. Med. Biol. **48**, 3977–4000 (2003).

[12]J. Fan, W. Luo, E. Fourkal, T. Lin, J. Li, I. Veltchev, and C. Ma, "Shielding design for a laser-accelerated proton therapy system," Phys. Med. Biol. **52**, 3913–3930 (2007).

[13]S. Schell and J. J. Wilkens, "Modifying proton fluence spectra to generate spread-out Bragg peaks with laser accelerated proton beams," Phys. Med. Biol. **54**, N459–N466 (2009).

[14]R. L. Siddon, "Calculation of the radiological depth," Med. Phys. **12**, 84–87 (1985).

[15]T. Haberer, W. Becher, D. Schardt, and G. Kraft, "Magnetic scanning system for heavy ion therapy," Nucl. Instrum. Methods Phys. Res. A **330**, 296–305 (1993).

[16]T. Bortfeld, "An analytical approximation of the Bragg curve for therapeutic proton beams," Med. Phys. **24**, 2024–2033 (1997).

[17]L. Kaufman and P. J. Rousseeuw, *Finding Groups in Data: An Introduction to Cluster Analysis*, Wiley Series in Probability and Mathematical Statistics (Wiley, New York, 1990).

[18]A. Lomax, "Intensity modulation methods for proton radiotherapy," Phys. Med. Biol. **44**, 185–205 (1999).

[19]N. Kanematsu, M. Endo, Y. Futami, T. Kanai, H. Asakura, H. Oka, and K. Yusa, "Treatment planning for the layer-stacking irradiation system for three-dimensional conformal heavy-ion radiotherapy," Med. Phys. **29**, 2823–2829 (2002).

[20]U. Oelfke and T. Bortfeld, "Inverse planning for photon and proton beams," Med. Dosim. **26**, 113–124 (2001).

[21]J. J. Wilkens, J. R. Alaly, K. Zakarian, W. L. Thorstad, and J. O. Deasy, "IMRT treatment planning based on prioritizing prescription goals," Phys. Med. Biol. **52**, 1675–1692 (2007).

[22]D. Pflugfelder, J. J. Wilkens, S. Nill, and U. Oelfke, "A comparison of three optimization algorithms for intensity modulated radiation therapy," Z. Med. Phys. **18**, 111–119 (2008).

[23]J. O. Deasy, A. I. Blanco, and V. H. Clark, "CERR: A computational environment for radiotherapy research," Med. Phys. **30**, 979–985 (2003).

[24]B. Gottschalk, A. M. Koehler, R. J. Schneider, J. M. Sisterson, and M. S. Wagner, "Multiple Coulomb scattering of 160 MeV protons," Nucl. Instrum. Methods Phys. Res. B **74**, 467–490 (1993).

[25]L. Hong, M. Goitein, M. Bucciolini, R. Comiskey, B. Gottschalk, S. Rosenthal, C. Serago, and M. Urie, "A pencil beam algorithm for proton dose calculations," Phys. Med. Biol. **41**, 1305–1330 (1996).

[26]D. M. Shepard, M. A. Earl, C. X. Yu, and Y. Xiao, in *Intensity-Modulated Radiation Therapy: The State of the Art*, edited by J. R. Palta and T. R. Mackie (Medical Physics, Madison, 2003), pp. 115–137.